Front. Optoelectron. 2018, 11(1): 60–68
https://doi.org/10.1007/s12200-018-0761-9

RESEARCH ARTICLE

Use of fiber Bragg grating sensors for monitoring delamination damage propagation in glass-fiber reinforced composite structures

Ayad KAKEI[1,2,3], Jayantha A. EPAARACHCHI (✉)[1,2]

1 School of Mechanical and Electrical Engineering, University of Southern Queensland, Toowoomba QLD 4350, Australia
2 Centre for Future Materials, University of Southern Queensland, Toowoomba QLD 4350, Australia
3 University of Kirkuk, College of Engineering, Kirkuk, Iraq

Abstract Embedded fiber Bragg grating (FBG) sensors have been widely used for damage monitoring of fiber composite structures for a few decades. However, many remaining engineering challenges have delayed FBG based *in situ* structural health monitoring (SHM) systems. One of the major problem associated with FBG based SHM system is the unavailability of reliable data processing algorithms. The present work details a study which has been undertaken for identification of delamination crack propagation in fiber reinforced polymer (FRP) composite plate under uniaxial loading. The strain measured by embedded FBG sensors closer to the crack tip was used to qualitatively and quantitatively analyze delamination damage propagation using recently proposed elasto-plastic model. Strain energy release rate was calculated and compared with the model prediction. The study has concluded that the delamination crack propagation in a FRP composite can be monitored successfully using an integral approach of FBG sensors measurements and the predictions of proposed elasto-plastic model.

Keywords fiber Bragg grating (FBG) sensors, composite, damage modelling, fracture energy

1 Introduction

Glass fiber reinforced polymer (GFRP) composites have been widely used as structural components in various branches of mechanical engineering, such as automotive and aerospace, due to their excellent mechanical properties and superior strength to weight ratio. Due to increased use of GFRP materials for manufacturing of structural component, the damage evaluation of GFRP structures has gradually became an urgent research area during recent years. There are many remaining unresolved areas of damage evaluation of composite materials. The separation of two bonded plies –i.e., delamination damage is one of the remaining unresolved critical failure modes of GFRP. In particular, delamination in frequently use GFRP material such as woven composite (WC) reinforced polymers has harmful effects on structural integrity [1,2]. As such, in-depth understanding of delamination crack mechanisms is essential to fill the gaps in fundamental knowledge required for structural durability and damage tolerance evaluation of this class of textile reinforced materials [2]. Unfortunately, a limited research work have been done to date on textile woven materials and their delamination fracture toughness measurements [3].

The critical strain energy release rate (CSERR) or critical delamination fracture energy (G_C) is the most used parameter to predict the delamination behavior of the laminated composite structures [4]. Shokrieh and Heidari-Rarani [5] have studied the effect of laminae stacking sequence on R-curve behavior of E-glass/epoxy laminated composites. The result shows that stacking sequence has no effect on the fiber bridging length in double cantilever beam (DCB) specimen. Shokrieh et al. [6] have declared that R-curves are almost remain constant in the size range of $8.5 < a_0/h < 19$ (a_0–initial crack length, h-plate thickness), i.e., it depends on the size and geometry of specimen. Due to these findings, it has been declared that R-curve may no longer be used as composite laminates characterization. However, at this a normalized relation G/G_C (at initiation and propagation of delamination processes) can be used as a part of a material database to

Received September 29, 2017; accepted December 26, 2017

E-mail: jayantha.epaarachchi@usq.edu.au

predict the delamination crack growth behavior. Ghasemnejad et al. [7] have investigated the effect of delamination crack growth of hybrid box structures on energy absorption. The critical fracture energy modes I and II (G_{IC} and G_{IIC}) of delamination at the crack initiation are more dominant than that of delamination propagation due to the energy absorption mechanism. However, the analysis and prediction of delamination initiation and propagation is too complex [8,9], and therefore delamination damage predication needs a reliable technique to capture the delamination damage before propagating.

Embedment of fiber Bragg grating (FBG) sensors in composite structures appears to be a highly innovative and promising method for detecting important process defects at early stage and delamination damage propagation. The reflected spectrum of a Bragg grating can provide an important information concerning the solidification shrinkage strains developed during the curing process [10,11] and *in-situ* and in real-time monitoring of strain fields build up during the fabrication procedure of structures such as the fused deposition modelling (FDM) technology [12,13]. As stated above, these strains can induce inner strains when accumulated in the structure can give rise to delamination crack [14]. Detection and evaluation of crack damage modes of laminated composite materials using FBG sensor have been investigated by many researchers. Yashiro et al. [15] have tried to link the multiple damage states of the laminate directly to the complicated reflection spectrum of the FBG sensor in a numerical model to obtain detailed strain distributions around the damaged region. The results show that the proposed approach is suitable for predicting multiple damage states in composite laminates. Sans et al. [16] have used long FBG sensor to indicate the crack tip location in carbon/epoxy unidirectional samples which were subjected to mixed-mode bending. Long FBG sensors can obviously detect crack tip inside the specimen. Okabe and Yashiro [17] have used embedded FBG sensor in order to detect damage in holed CFRP laminated under static and cyclic loading. Kahandawa et al. [18,19] have used FBG sensors to monitor and quantify the damage of glass fiber reinforced composites. Those researches have shown that the spectrum shape did not change during fatigue loading but it did change during the static loading. Takeda et al. [20] have investigated the quantitative detection of delamination in CFRP cross-ply laminates under four-point bending test loading using the small-diameter FBG sensor. They have suggested that the intensity ratio in the spectrum as an effective indictor for the prediction of the delamination length. In an another study, Takeda et al. [21] have applied small-diameter FBG sensors for monitoring of delamination size in the CFRP laminates subjected to a low-velocity impact. Their results have shown that the small-diameter FGB sensors are successful for monitoring and evaluation of the delamination in laminated composites. Kakei et al. [22] have presented an elasto-plastic theory for evaluating Mode I delamination damage growth in woven glass fiber/epoxy composites. The strain measured by an embedded FBG sensor was used for model prediction. The predictions were validated using experimental observations. This study also have proved the potential of FBG for monitoring delamination. Ling et al. [23,24] have monitored mode II damage behavior of beams manufactured with woven composite laminate and having purposely created number of delaminations along the beam's axis, using embedded FBG sensors. The delamination propagation were investigated using end notch flexure (ENF) tests. The results have shown that in delamination case, the reflection spectrum is fully destroyed due to the interaction between the FBG and the delamination at the applied load. Stutz et al. [25] used an array of several short FBG sensors to measure local strains close to the crack plane. The measured strain serves to determine the tractions in the bridging zone in monotonic and fatigue loads.

The aim of the present work is to use newly established elasto-plastic model to evaluate delamination damage behavior in 0/90 woven composite using the strain at the crack tip that measured by an embedded FBG sensor.

2 Integrated approach of damage sensing and modeling

In this study, embedded FBG sensor strain reading have been incorporated with recently proposed [22] elasto-plastic model. The analysis assumes that elastic behavior in the orthotropic laminate and the plastic behavior of the epoxy in laminate at the tip of delamination (matrix), as shown in Fig. 1.

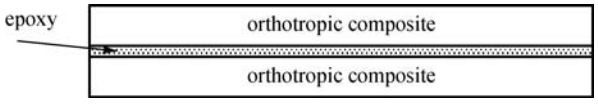

Fig. 1 Schematic representation of composite beam (section $b \times h$) as two different materials, elastic orthotropic composite, and the elastic epoxy layer of a negligible thickness. b is width of the specimen; h is thickness of the specimen

Due to local bending at the crack front [26], plastic deformation is assumed at the significantly thin inter-laminar region (epoxy) near the crack tip at the distance equal to X. The threshold delamination crack length $a = X_Y$, where X_Y is distance to crack tip from left end of the plate, as shown in Fig. 2.

The energy input have estimated E_{total}, and is considered the energy balance for increment of the crack growth, Δa, associated with a simultaneous increase in Δv, the normal distance of the extremity of the composite beam from the initial plane [27]

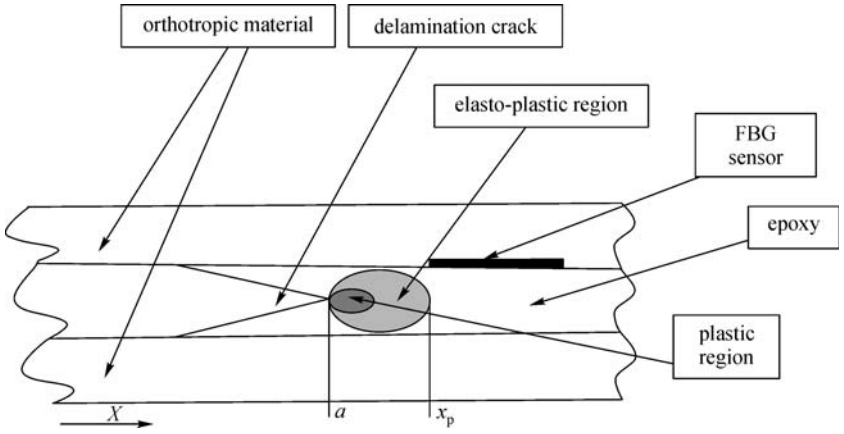

Fig. 2 Schematic representation of beam, the section near the crack front is in the elastoplastic

$$G_C = \frac{p}{b}\frac{\partial v}{\partial a} - \frac{1}{b}\frac{\partial E_{total}}{\partial a}. \quad (1)$$

As the applied load is normal to the shear plane, shear force Q is equal to zero. Then the fracture energy is equal to the energy absorbed by the displacement (v) of the composite beam, Eq. (2) can be written as

$$G_C = -\frac{1}{b}\frac{\partial E_{total}}{\partial a}. \quad (2)$$

Let the region at tip of the delamination crack is plastic and the effect of delamination crack region is elasto-plastic as shown in Fig. 2. The region near the tip of delamination crack can be assumed perfectly plastic and the material status at the transforms to elasto-plastic. The total energy expended per unit length of composite beam with crack delamination, e_{total} is [22]

$$e_{total} = e_S + e_e = b\left(\frac{E_{ep}\varepsilon_Y h^2}{8R} - \frac{hE_{ep}\varepsilon_Y^2}{4} + \frac{ER\varepsilon_{max}^3}{3}\right), \quad (3)$$

where E is the young modulus of composite specimen, E_{ep} is Young modulus of epoxy (matrix), ε_{max} is the maximum strain measured in the surface of composite specimen using strain gauge, ε_Y is the yield strain of epoxy measured in the matrix of composite specimen using FBG sensor, e_e is elastic energy due to structural changes/ or dissipated from delamination crack and e_S is elastic stored energy per unit length of composite beam (along direction x with a perfect elastic condition). The main concern is about the range $a < x \leqslant x_p$ as shown in Fig. 2, where the combined elastic and plastic deformation exists due to delamination crack at the interface. Integrating over the length range of x, the total energy input, E_{total} in the composite beam

$$E_{total} = E_0 + \int_a^{x_p} e_{total} dx. \quad (4)$$

Let a moment develops in the section due to delamination crack which works as a hard point in the section, then total moment on the section is given by [22]

$$M = \frac{bE_{ep}\varepsilon_Y h^2}{4} + \frac{2bE\varepsilon_{max}^3 R^2}{3} - \frac{bE_{ep}\varepsilon_Y^2 R^2}{3}. \quad (5)$$

As a result, the relative displacement between crack surfaces causes shear strain at the matrix (epoxy) in the composite. The axial force produces a crack-tip sliding displacement or only causes mode II delamination damage. The crack-tip sliding displacement depends on the thickness of the upper (h_1) and lower (h_2) arms. then it can be assumed that the total input energy at the crack plane system is equal to the difference between input energy at upper and lower arms of the plate, then, Eq. (2) can be written as

$$G_C = -\frac{1}{b}\left[\left(\frac{\partial E_{total}}{\partial a}\right)_{upper} - \left(\frac{\partial E_{total}}{\partial a}\right)_{lower}\right]. \quad (6)$$

3 Use of FBG sensor for damage prediction

The principle of the FBG sensor is based on the measurement of the changes in reflected signal, which is the center wavelength of back-reflective light from a Bragg grating. The spectral response of a uniform FBG in its free state is a signal peak centered at the Bragg wavelength λ_B as defined by the Bragg condition [28].

$$\lambda_B = 2n_{eff}\Lambda, \quad (7)$$

where n_{eff} is the effective refractive index for the guided mode of interest and Λ is the constant nominal period of the refractive index modulation. When a mechanical deformation (strain) is subjected onto grating, it will change the effective index of refraction as well as the periodic spacing index. The Bragg wavelength shift caused by the change of strain can be expressed in the form

$$\frac{\Delta\lambda_B}{\lambda_B} = \varepsilon P_e, \quad (8)$$

where P_e is the strain optic coefficient and it is calculated

as 0.789.

To identify the delamination cracks in the specimens, distortion index (*DI*) value is used. *DI* can be expressed as

$$DI = \frac{D_{si}}{D_{so}}, \tag{9}$$

where D_{si} is the current distortion and D_{so} is the distortion at the original condition (no loading). Distortion (D_S) can be expressed as

$$D_s = \frac{FWHM}{F}, \tag{10}$$

where F is the peak value of the FBG sensor reflection spectra, and *FWHM* is the full-width at half-maximum value of FBG spectra as shown in Fig. 3. Peak wavelength ratio (*PWR*) of FBG sensor is another expression, is used to evaluate delamination damage and it can be expressed as

$$PWR = \frac{F_i}{F_{io}}, \tag{11}$$

where F_i is the current peak wavelength and F_{io} is the peak wavelength at the original condition (no loading). These phenomenon (*DI* and *PWR*) can be used to identify the presence of delamination damage in the composite specimens.

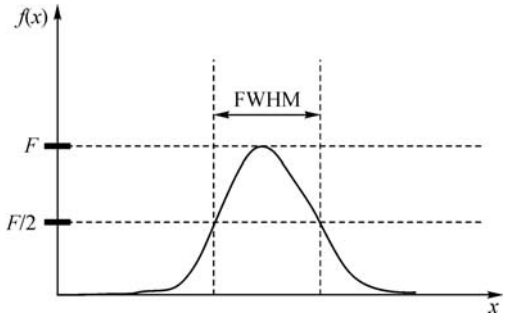

Fig. 3 Full-width at half-maximum (FWHM)

4 Experimentation

The material examined in the present work was a 15-layer (0/90) AR 145 E-glass woven roving (398 g/m^2 weight and 0.5 mm thickness) fiber-reinforced epoxy resin matrix. Kenetix R246TX epoxy resin is used as the matrix material. The plain weave structure of the woven cloth laminate consists of two mutually orthogonal directions (warp and weft) with an approximate glass volume fraction of 60%. An artificial delamination 50 mm × 40 mm in size was made at a particular layer locations through the thickness, by embedding Teflon paper (0.001 mm thickness) during manufacture. An optical fibers with grating length 5 mm and Bragg wavelength λ_B = (1548±0.3) nm was embedded between the layers above the purposely created delamination. The FBG was located approximately (10±1) mm from the delamination crack tip. The sensor location was carefully selected to keep the maximum sensitivity of the sensor to receive changes at the damage front. One large specimen was manufactured and then cut into smaller rectangular 400 mm × 40 mm coupons. A few uniaxial strain gauges (FLA-5-11-1L) were bonded in the surface of specimens in different places to measure change the strain on the surface. The strain gauges are numbered as shown in Fig. 4. Strain gauge 1 was bonded at 10 mm from the end of delamination (embedded FBG sensor is located directly underneath), strain gauge 2 was bonded on the delamination area, and strain gauge 3 was bonded at 55 mm from end of initial delamination.

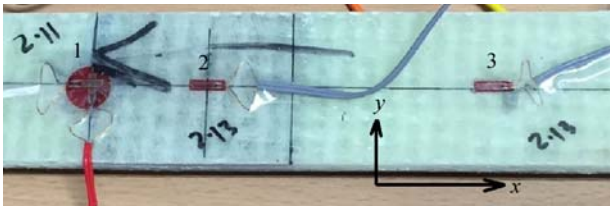

Fig. 4 Strain gauge locations on the sample surface (FBG sensor embedded between two layers and align with strain gauge 2 through the thickness)

All tests were conducted on MTS 810 100 kN uniaxial testing machine fitted with hydraulic grips. The test specimen was attached to MTS 810 machine with approximately 50 mm of gripped at each end. The tensile load was increased incrementally from 2 to 35 kN. Each increase in the load was applied under displacement control at a rate of 1.5 mm/min. The test setup is shown in Fig. 5. During load application, the reflected spectra of the FBG sensor were recorded using a micron optics interrogator (sm-125) for post processing.

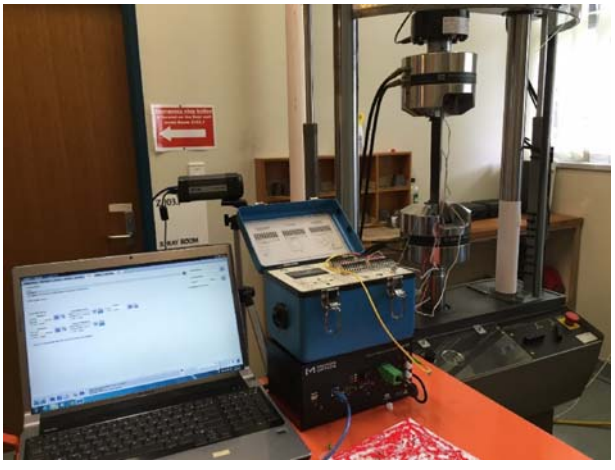

Fig. 5 Experimental setup

5 Results and discussion

With the increasing tensile load on the sample strain

measured at strain gauges 1 and 3 had shown initial linear response and transformed to nonlinear response as shown in Fig. 6. Both strain gauges show the same strain at linear region as anticipated. After 25 kN applied load, increase of damage area may have occurred in the composite specimen at the region between strain gauges 1 and 3 leadings to sharp increase in the strain measured by strain gauges 1 and 3. Simultaneously, with the increased loads has caused the nonlinear strain behavior in strain gauge 2. This nonlinearity may be attributed to delamination underneath the strain gauge 2 which caused extended de-bond between layers. This observation has confirmed the extent of delamination which caused the significant changes in the strain measurements. As shown in Fig. 6, measured strain from gauge 2 was lesser than measured strains by strain gauges 1 and 3. This difference may be an indication of local bending at the middle of the delamination area due to hard point of delamination crack tip. The stress-strain behavior transformed to nonlinear after 5 kN applied loading.

The distortion of FBG spectrum occurs due to the effect of non-uniform strain at the tip of delamination crack when the delamination crack tip reaches FBG sensor region [28]. Figure 7 shows the changing and shifting of FBG spectrums with the advancement of delamination cracks. Initially the spectrum of FBG sensor shows the uniform strain at the location of sensor. Significant changes in FBG spectrum can be seen at 15 kN applied load, indicating the reach of crack tip closer to FBG sensor. Finally the FBG spectrums have shown a significant distortion when applied load reach 20 kN mark. This distortion is due to non-uniform (plastic) strain field around the crack tip.

The changed reflectivity of the embedded FBG sensor was simulated using FBG SiMul V1.0 software [29]. FBG SiMul V1.0 was used as a tool to study the implementation of FBG sensors solutions in any subjectively loaded structure as shown in Fig. 8. This software is designed as an interface program to calculate longitudinal strain at FBG sensor region from ABAQUS software and then calculate distortion in the FBG sensor spectrum.

In this case, the delamination damage was perfectly a mode II delamination because there is no space for crack opening. Critical delamination fracture energy G_C of WC/epoxy is equal to 1.05 mJ [26]. Delamination damage keep propagating when the delamination fracture energy (G) is equal to critical delamination fracture energy (G_C) or the delamination fracture energy (G/G_C) equal to 1. As shown in the Fig. 9, delamination onset strains were measured by embedded FBG sensor. If the ratio G/G_C is greater than 1, the crack status becomes unstable. As such, G/G_C-strain curve shown in Fig. 9 is providing a significant index for evaluating delamination damage stability for laminated composite materials under uniform tensile loadings.

The distortion of FBG sensor spectrum with the applied loads provides an index to detect delamination damage in the laminated composite structures. Two parameters *DI* and *PWR* (Eqs. (9) and (11), respectively) were used to evaluate delamination damage growth and elasto-plastic region in the matrix with applied loads (Fig. 10). Both parameters were equal to unity before 4 kN applied load. Significant changes were noticed in both parameters during the increase of loads from 4 to 15 kN. This behavior was

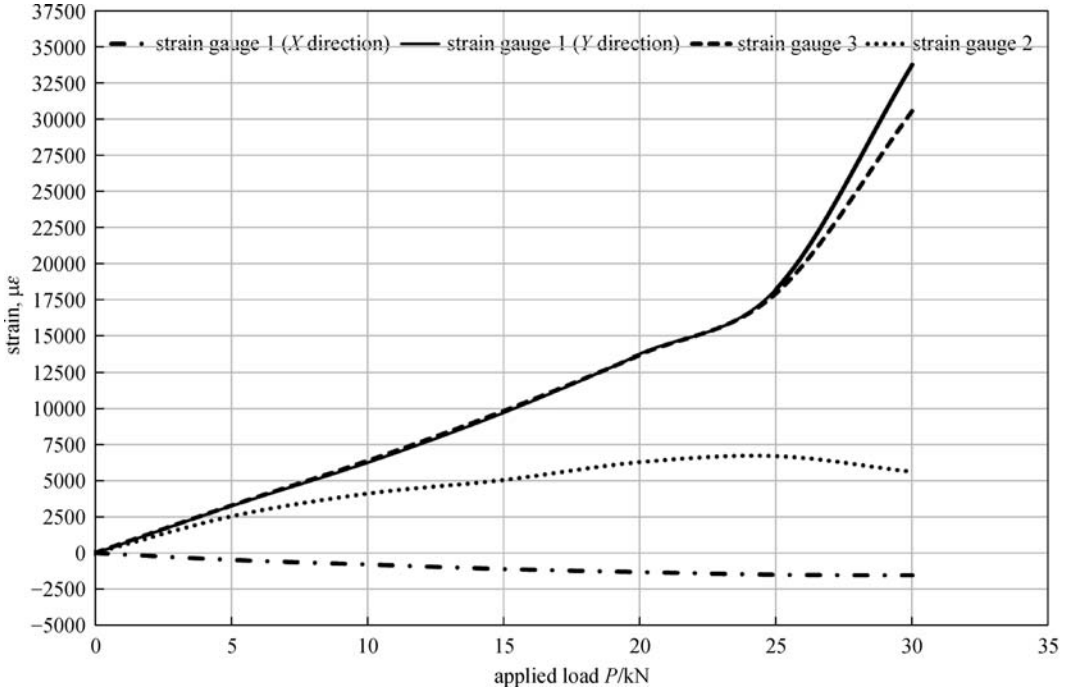

Fig. 6 Effect of delamination location on the strain gauges reading

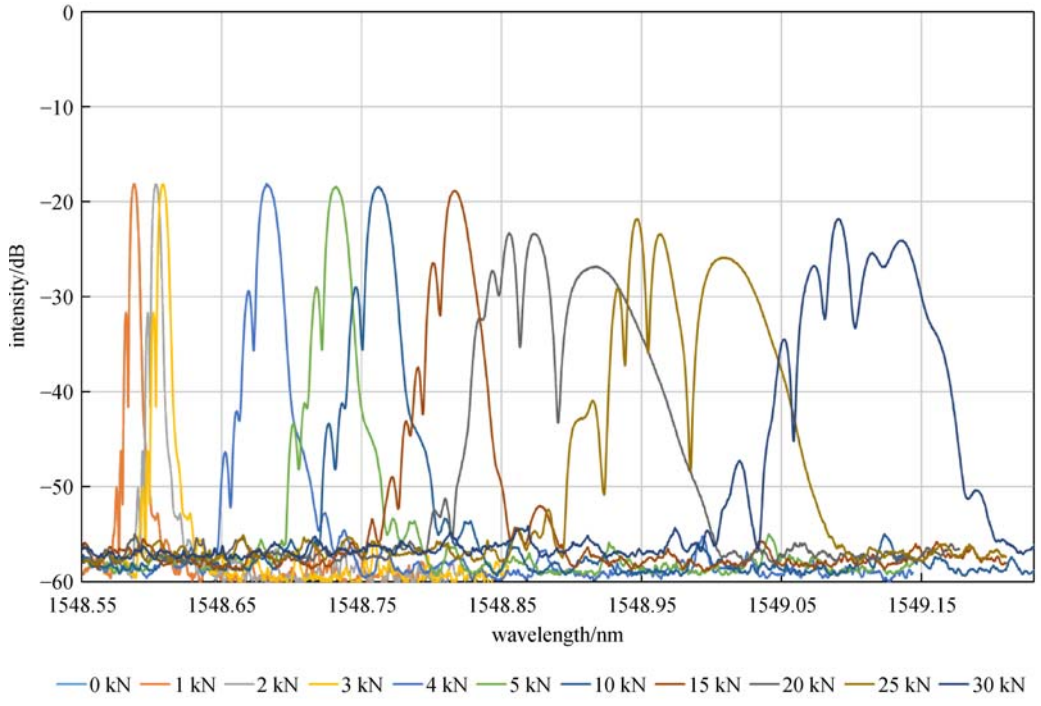

Fig. 7 Spectra of embedded FBG in WC/epoxy specimen under tensile loading (delamination test) with increasing applied loadings (experimental result)

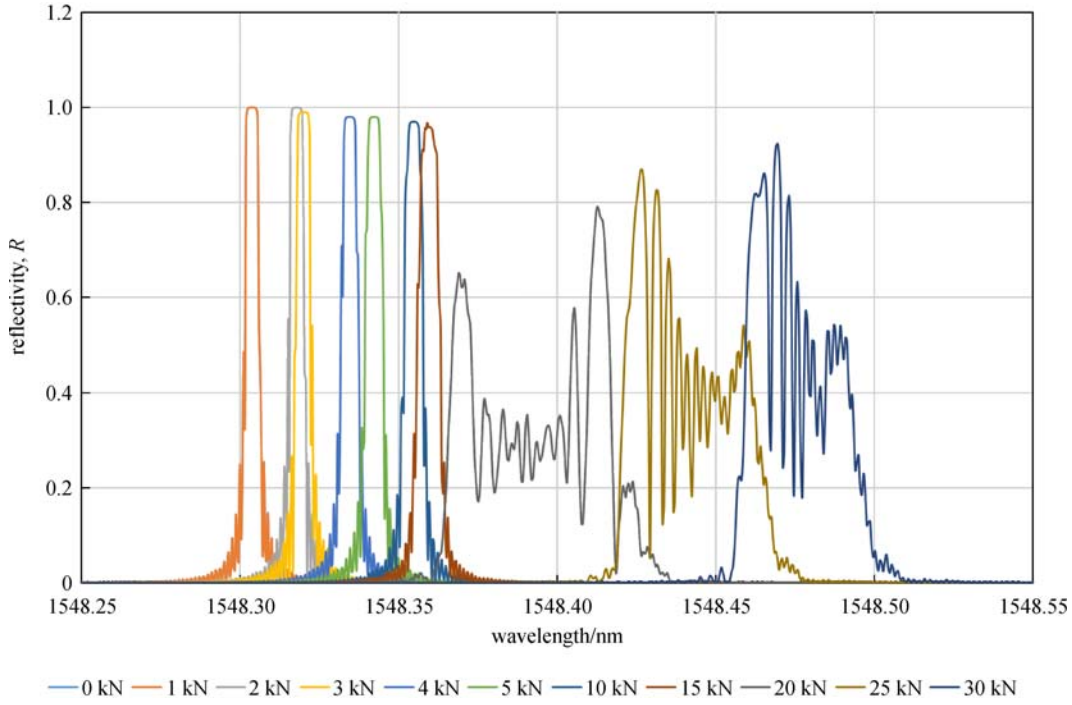

Fig. 8 Spectra of embedded FBG in WC/epoxy specimen under tensile loading (delamination test) with increasing applied loads, using FBG_SiMul V1.0 software

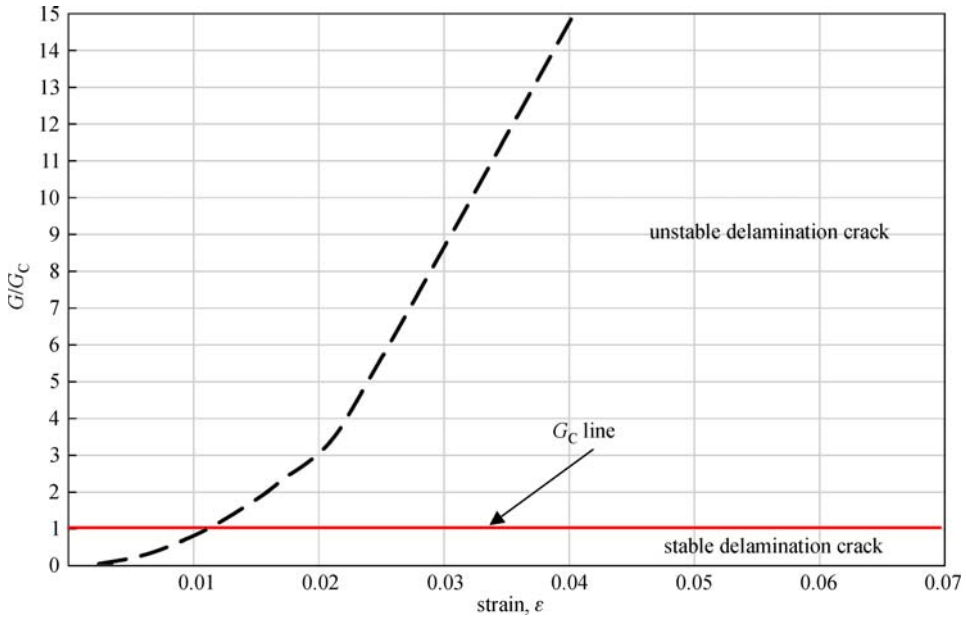

Fig. 9 Examination of delamination stability on the G/G_C ratio

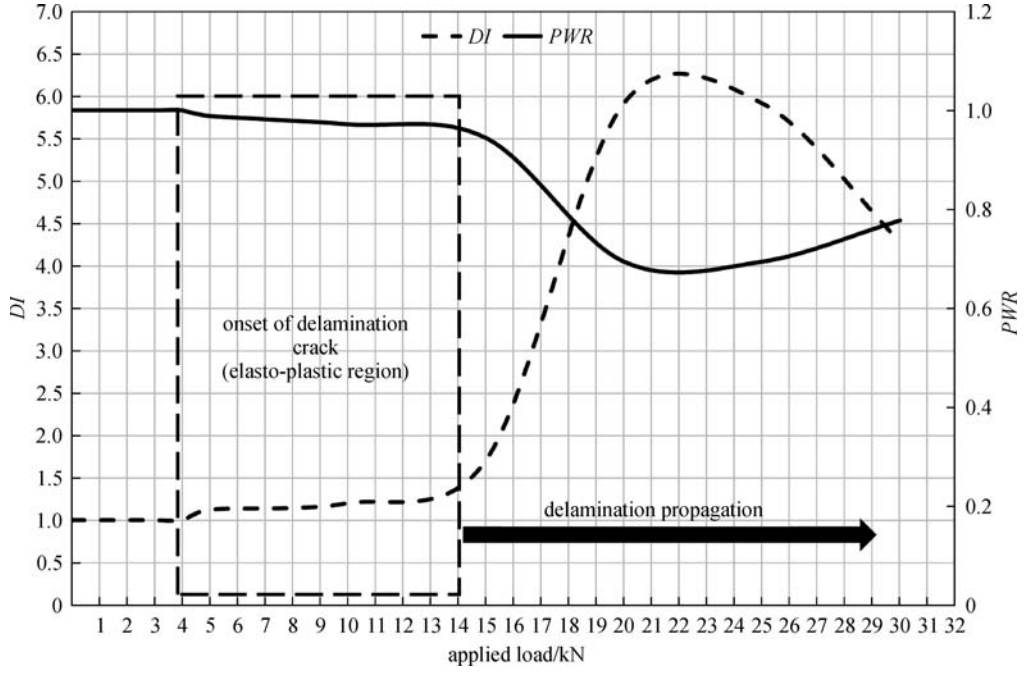

Fig. 10 Detection of delamination crack onset and propagation for WC/epoxy under tensile loadings using both *DI* and *PWR* parameters (experimental results)

due to the initiation of elasto-plastic region at the delamination crack tip during the propagation of the crack. The index *DI* and *PWR* were remaining at unity when the delamination crack tip is perfectly elastic. Once the tip of delamination crack changes from elastic to elasto-plastic region, the stress concentration at the crack tip causes the distortion of FBG sensor as shown in Fig. 7. The distortion in FBG spectrum from the onset of crack confirms the elasto-plastic state in the epoxy (matrix) at the crack tip. This significantly high strain possibly caused by the crack which was propagating through the gratings region of FBG sensor. The strain values became stables again when the crack pass the FBG sensor. The changing of FBG sensor spectrum has provided excellent prediction

and evaluation of initiation and propagation of delamination damage but it could not calculate clearly the size of delamination damage in the WC/epoxy specimens.

6 Conclusion

An embedded FBG sensor was used to measure strain inside a WC $(0/90)_{15}$ test specimen under uniaxial loading. The change in the FBG spectra was monitored and the strain at FBG location was estimated from this response. The distortion of FBG spectra was observed due to non-uniform strain at the tip of delamination crack which was at elasto-plastic state. The strain measured by FBG sensor were used to calculate fracture energy by recently proposed elasto-plastic model. Further, the indicators *DI* and *PRW* were calculated to evaluate onset and stability of delamination crack. The result showed that both parameters have provided accurate indications of delamination damage, such as stability and instability of the crack. As such FBG sensor has shown its potential for monitoring the on-set and the propagation of delamination.

Acknowledgements Authors like to acknowledge the technical support provided by Mr. Mohan Trada, School of Mechanical and Electrical Engineering and Mr. Wayne Crowell, Centre for Future Materials of USQ.

References

1. Kakei A, Epaarachchi J, Mainul M, Leng J. Development of fracture and damage modeling concepts for composite materials. In: Epaarachchi J, Kahandawa G, eds. Structural Health Monitoring Technologies and Next-Generation Smart Composite Structures. 2016, Roca Raton: CRC Press, 339–364
2. Kuhtz M, Hornig A, Gude M, Jäger H. A method to control delaminations in composites for adjusted energy dissipation characteristics. Materials & Design, 2017, 123: 103–111
3. Olave M, Vara I, Usabiaga H, Aretxabaleta L, Lomov S V, Vandepitte D. Nesting effect on the mode II fracture toughness of woven laminates. Composites Part A, Applied Science and Manufacturing, 2015, 74: 174–181
4. Shokrieh M M, Zeinedini A, Ghoreishi S M. On the mixed mode I/II delamination R-curve of E-glass/epoxy laminated composites. Composite Structures, 2017, 171: 19–31
5. Shokrieh M M, Heidari-Rarani M. Effect of stacking sequence on R-curve behavior of glass/epoxy DCB laminates with 0°//0° crack interface. Materials Science and Engineering A, 2011, 529: 265–269
6. Shokrieh M M, Heidari-Rarani M, Ayatollahi M R. Delamination R-curve as a material property of unidirectional glass/epoxy composites. Materials & Design, 2012, 34: 211–218
7. Ghasemnejad H, Hadavinia H, Aboutorabi A. Effect of delamination failure in crashworthiness analysis of hybrid composite box structures. Materials & Design, 2010, 31(3): 1105–1116
8. Yasaee M, Bigg L, Mohamed G, Hallett S R. Influence of Z-pin embedded length on the interlaminar traction response of multi-directional composite laminates. Materials & Design, 2017, 115: 26–36
9. Shaoquan W, Shangli D, Yu G, Yungang S. Thermal ageing effects on mechanical properties and barely visible impact damage behavior of a carbon fiber reinforced bismaleimide composite. Materials & Design, 2017, 115: 213–223
10. Chang F K.Structural Health Monitoring. Lancaster: DESTechnol Publications, 2003
11. Vieira A, de Oliveira R, Frazão O, Baptista J M, Marques A T. Effect of the recoating and the length on fiber Bragg grating sensors embedded in polymer composites. Materials & Design, 2009, 30(5): 1818–1821
12. Kousiatza C, Karalekas D. *In-situ* monitoring of strain and temperature distributions during fused deposition modeling process. Materials & Design, 2016, 97: 400–406
13. Kantaros A, Karalekas D. Fiber Bragg grating based investigation of residual strains in ABS parts fabricated by fused deposition modeling process. Materials & Design, 2013, 50: 44–50
14. Kanerva M, Antunes P, Sarlin E, Orell O, Jokinen J, Wallin M, Brander T, Vuorinen J. Direct measurement of residual strains in CFRP-tungsten hybrids using embedded strain gauges. Materials & Design, 2017, 127(Supplement C): 352–363
15. Yashiro S, Takeda N, Okabe T, Sekine H. A new approach to predicting multiple damage states in composite laminates with embedded FBG sensors. Composites Science and Technology, 2005, 65(3–4): 659–667
16. Sans D, Stutz S, Renart J, Mayugo J A, Botsis J. Crack tip identification with long FBG sensors in mixed-mode delamination. Composite Structures, 2012, 94(9): 2879–2887
17. Okabe T, Yashiro S. Damage detection in holed composite laminates using an embedded FBG sensor. Composites Part A, Applied Science and Manufacturing, 2012, 43(3): 388–397
18. Kahandawa G C, Epaarachchi J, Wang H, Canning J, Lau K T. Extraction and processing of real time strain of embedded FBG sensors using a fixed filter FBG circuit and an artificial neural network. Measurement, 2013, 46(10): 4045–4051
19. Kahandawa G C, Epaarachchi J A, Wang H, Followell D, Birt P. Use of fixed wavelength fibre-Bragg grating (FBG) filters to capture time domain data from the distorted spectrum of an embedded FBG sensor to estimate strain with an artificial neural network. Sensors and Actuators A, Physical, 2013, 194: 1–7
20. Takeda S, Okabe Y, Takeda N. Delamination detection in CFRP laminates with embedded small-diameter fiber Bragg grating sensors. Composites Part A, Applied Science and Manufacturing, 2002, 33(7): 971–980
21. Takeda S, Minakuchi S, Okabe Y, Takeda N. Delamination monitoring of laminated composites subjected to low-velocity impact using small-diameter FBG sensors. Composites Part A, Applied Science and Manufacturing, 2005, 36(7): 903–908
22. Kakei A A, Islam M,Leng J,EpaarachchiJ. Use of an elasto-plastic model and strain measurements of embedded fibre Bragg grating sensors to detect Mode I delamination crack propagation in woven cloth (0/90) composite materials. Structural Health Monitoring, 2017, doi:10.1177/1475921717694812

23. Ling H Y, Lau K, Cheng L, Su Z. Mode II fracture behaviour monitoring for composite laminates using embedded fibre Bragg grating sensors. Composite Structures, 2006, 76(1–2): 88–93
24. Ling H Y, Lau K T, Su Z, Wong E T T. Monitoring mode II fracture behaviour of composite laminates using embedded fiber-optic sensors. Composites Part B, Engineering, 2007, 38(4): 488–497
25. Stutz S, Cugnoni J, Botsis J. Studies of mode I delamination in monotonic and fatigue loading using FBG wavelength multiplexing and numerical analysis. Composites Science and Technology, 2011, 71(4): 443–449
26. Kakei A, Epaarachchi J A, Islam M, Leng J, Rajic N. Detection and characterisation of delamination damage propagation in woven glass fibre reinforced polymer composite using thermoelastic response mapping. Composite Structures, 2016, 153: 442–450
27. Chauffaille S, Jumel J, Shanahan M E R. Elasto-plastic analysis of the single cantilever beam adhesion test. Engineering Fracture Mechanics, 2011, 78(13): 2493–2504
28. Sorensen L, Botsis J, Gmür T, Cugnoni J. Delamination detection and characterisation of bridging tractions using long FBG optical sensors. Composites Part A, Applied Science and Manufacturing, 2007, 38(10): 2087–2096
29. Pereira G, McGugan M, Mikkelsen L P.FBG_SiMul V1.0: Fibre Bragg grating signal simulation tool for finite element method models. SoftwareX

Dr. **Jayantha A. Epaarachchi** is a senior academic attached to School of Mechanical and Electrical Engineering, University of Southern Queensland (USQ), Australia. His major research interests are smart composite structures, structural health monitoring (SHM), fatigue, fracture, and damage mechanics of fibre reinforced composite materials. He is an active member of Centre for Future Materials (CFM), USQ. He has published over 80 scientific papers, three book chapters and edited a book & special issues of journals. Dr. Epaarachchi owns an US patient on SHM with Boeing Aircraft Company and completed a few large scale SHM and smart composite structures projects. He was a visiting scientist at University of Bristol, UK and Harbin Institute of Technology, China.